

Photoresistivity and optical switching of graphene with DNA lattices

Atul Kulkarni^{a,b,1}, Rashid Amin^{b,c,1}, Hyeongkeun Kim^{b,d}, Byung Hee Hong^{b,d}, Sung Ha Park^{b,c,*}, Taesung Kim^{a,b,**}

^aSchool of Mechanical Engineering, Sungkyunkwan University, Suwon 440-746, Republic of Korea

^bSungkyunkwan Advanced Institute of Nanotechnology (SAINT), Sungkyunkwan University, Suwon 440-746, Republic of Korea

^cDepartment of Physics, Sungkyunkwan University, Suwon 440-746, Republic of Korea

^dDepartment of Chemistry, Sungkyunkwan University, Suwon 440-746, Republic of Korea

ARTICLE INFO

Article history:

Received 18 June 2011

Received in revised form

15 August 2011

Accepted 9 September 2011

Available online 2 October 2011

Keywords:

DNA

Self-assembly

Lattice

Graphene

Photoresistivity

Optical switch

ABSTRACT

We present the photon induced conductivity of 2D DNA lattices with and without graphene and demonstrate the switching current responses controlled by light irradiation. The conductivity in the DNA lattices with protein streptavidin controlled by blue and white lights shows significant enhancement with the addition of graphene. An optical pulse response of a graphene immobilized DNA lattice is encouraging and may lead to various bio-sensing applications such as immunological assays, DNA forensics, and toxin detection.

© 2011 Elsevier B.V. All rights reserved.

There is motivation in the scientific community to fabricate advanced nano-bio interfaces for a variety of applications in the fields of biomedicine [1], bio-actuated devices [2,3], bio-detection [4,5], and clinical diagnostics [6,7]. The existing generation of active nano-bio devices is rooted in zero-dimensional (0D) nanoparticles, one-dimensional (1D) nanowires [8], and two-dimensional (2D) networks [9] that have shown excellent detection and interfacing abilities for both micro and nano molecular bio-components. However, the incompatibility in macroscale devices or sensors makes it challenging to apply these nanostructures for building interfaces with larger sized microorganisms or for retaining them on their respective networks.

Structural DNA nanotechnology [10–19] has opened the door for interdisciplinary research and development in nano-bio science. Particularly, the unique feature of DNA self-assembly is surrounded by multiple disciplines such as physics, chemistry, biology, material

science, medicine and even in computer science. DNA nanotechnology exploits the predictable self-assembly of DNA oligonucleotides for designing and constructing innovative and distinctive nanostructures that are valuable tools for numerous multidisciplinary applications. The supramolecular DNA architecture is composed of complementary base-pairs of adenine-thymine (A-T) and cytosine-guanine (C-G) based on specific hydrogen bonding. Because of the close stacking of base-pairs, consisting of purines and pyrimidines, quantum communication occurs in the π -stack region of the DNA molecule [20]. The conductivity mechanism in DNA is dominated by the transport of charge within the DNA strands [21]. A number of duplex DNA photoconductivity studies have been conducted to evaluate the electronic energy levels between DNA bases [22]. Here we present the photon induced conductivity of artificially designed DNA nanostructures with and without graphene and demonstrate the switching current–voltage (I – V) responses controlled by light irradiation.

A 2D double crossover biotinylated lattice (DX-BT) nanostructure is used to make the DNA-graphene interface. This DNA DX-BT nanostructure is assembled by two side-by-side double-stranded helices linked at two crossover junctions [23]. The unit DX-BT motif has a stiffness that is deficient in simple duplex DNA or in conventional branched junctions, signifying its suitability for being used in the periodic lattice assembly. A 2D DX-BT

* Corresponding author. Sungkyunkwan Advanced Institute of Nanotechnology (SAINT), Sungkyunkwan University, Suwon 440-746, Republic of Korea. Tel.: +82 31 299 4544; fax: +82 31 290 7055.

** Corresponding author. School of Mechanical Engineering, Sungkyunkwan University, Suwon 440-746, Republic of Korea.

E-mail addresses: sunhapark@skku.edu (S.H. Park), tkim@skku.edu (T. Kim).

¹ Contributed equally.

nanostructure composed of individual DX and DX-BT motifs is fabricated by programming the appropriate sticky ends and incorporating biotin protein in line with the DNA oligos' bases as shown in Fig. 1(a). A building block, a DX tile comprised of four strands of DNA, contributes to both helices. Each corner of all the DX units has a single-stranded sticky end with a distinctive sequence. We have

chosen the simplest non-trivial set of tiles to fabricate a 2D DX-BT lattice with a concentration of oligos of 200 nM. After annealing, the structure formation was verified by atomic force microscopy (AFM) shown in Fig. 1(c). The streptavidin (SA) protein binds to the biotin with high affinity in the DX-BT lattice, hence forth referred as DX-BT-SA. An equimolar concentration of SA was added to the

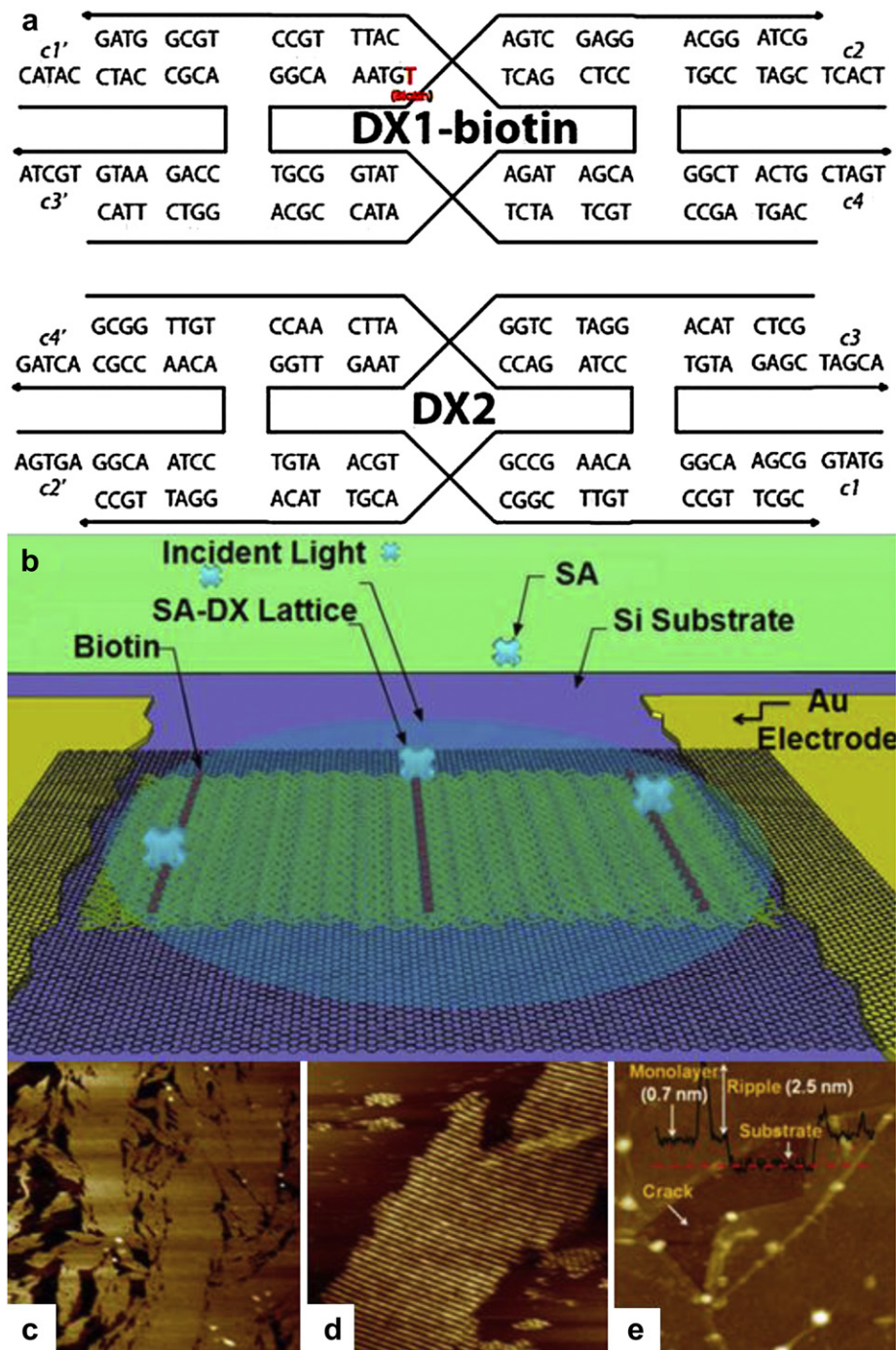


Fig. 1. A schematic of the DX-BT lattice structure ($1 \times 1 \mu\text{m}$) with SA binding to the biotin. (a) DNA base sequences for a DX-BT lattice. A biotinylated nucleotide, thymine is indicated in red. The complementary sticky end pairs are shown as c# and c#'. (b) The schematic illustration of the experiment setup. Graphene is layered onto the silicon oxide substrate in between and over the gold electrodes. Then the DX-BT lattice is immobilized on the graphene surface by adsorption. After $I-V$ evaluation, SA is pipetted onto the DX-BT lattice that binds to the biotin. (c) AFM image of the DX-BT lattice with a scan size of $1 \times 1 \mu\text{m}$. (d) AFM image of the DX-BT lattice after SA binding. The SA shows prominently in the image because of its comparatively larger diameter, $\sim 5 \text{ nm}$. (e) The contact-mode AFM image of the graphene film transferred onto SiO_2 . A few nm high ripples are usually formed due to the differences in thermal expansion of Cu and graphene and some cracks may appear during the transfer process. The height profile (red solid line) measured along the dashed red line indicates the thicknesses of mono- and bi-layers. (For interpretation of the references to color in this figure legend, the reader is referred to the web version of this article.)

DX-BT assembly on a graphene sheet, hence forth graphene is referred to as GP, for its I – V evaluation. The schematic illustration of the experimental setup is shown in Fig. 1(b) and representative AFM images of DX-BT, DX-BT-SA, and GP are shown in Fig. 1(c)–(e), respectively.

We have used a DX-BT lattice for the initial photon induced electrical conductance measurement. An optical fiber guided light source was placed above and focused using lens optics on the DX-BT film. A typical I – V behavior of the DX-BT lattice was measured in the dark and SA was added to the DX-BT lattice and again the I – V was observed, as illustrated in the Fig. 2(a) and (b). Subsequently, the DX-BT lattice was exposed to white light, with wavelengths ranging from 400 nm to 800 nm, and blue light with a wavelength of 460 nm. Fig. 2(a) describes the I – V response of the DX-BT nanostructure with white and blue light irradiation. After exposure to the radiation the rectifying behavior was observed shown in Fig. 2. It was found that the curves with enhanced positive current do not show a symmetrical shape. The average resistivity at 1 V is estimated to be $\rho_{\text{white}} = 7.14 \times 10^{12} \Omega \text{ m}$ and $\rho_{\text{blue}} = 16.66 \times 10^{12} \Omega \text{ m}$ with white and blue light irradiation, respectively. Interestingly, for DX-BT-SA, a noticeable conductivity change was observed with blue light irradiation as seen in Fig. 2(b). The estimated change in resistivity after adding SA is $\Delta\rho_{\text{blue}} = 7.6 \times 10^{12} \Omega \text{ m}$. Hence the resistivity decreased when the

DX-BT lattice was modified with streptavidin, under blue light irradiation. Lower resistivity of DX-BT-SA may come from structural alignment of periodic biomolecules although the SA proteins do not provide free electrons.

The exceptional photoconductivity of a bulk film of graphene sheets has been reported [24]. It is observed that the photoconductivity of graphene is increased with an increase in light intensity or an external electric field of the equivalent photon energy. Theoretically, the photoconductivity of graphene should be fairly strong because the intrinsic properties of graphene exhibit a maximum of the dark resistance [25]. A similar phenomenon was observed with graphene and DX-BT/DX-BT-SA complexes as shown in Fig. 2(c). Due to the different electrical properties of graphene and DNA, it is found that the flow of current is decreased after immobilization of the DX-BT lattices on graphene. This is opposite to the current flow through the DX-BT and DX-BT-SA lattices in the absence of graphene especially with blue, in the nanoampere (nA) range, and has a rectifying response, whereas in the case of graphene the current is increased to milliamperes (mA). Hence, the estimated resistivity of GP-DX-BT is $\rho_{\text{white}} = 2.85 \times 10^8 \Omega \text{ m}$ for white and $\rho_{\text{blue}} = 3.84 \times 10^8 \Omega \text{ m}$ for blue light. After the addition of SA, for GP-DX-BT-SA, the resistivity changes to $\rho_{\text{white}} = 3.87 \times 10^8 \Omega \text{ m}$ and $\rho_{\text{blue}} = 4.54 \times 10^8 \Omega \text{ m}$. If we consider the change in current, caused by light irradiation of only graphene,

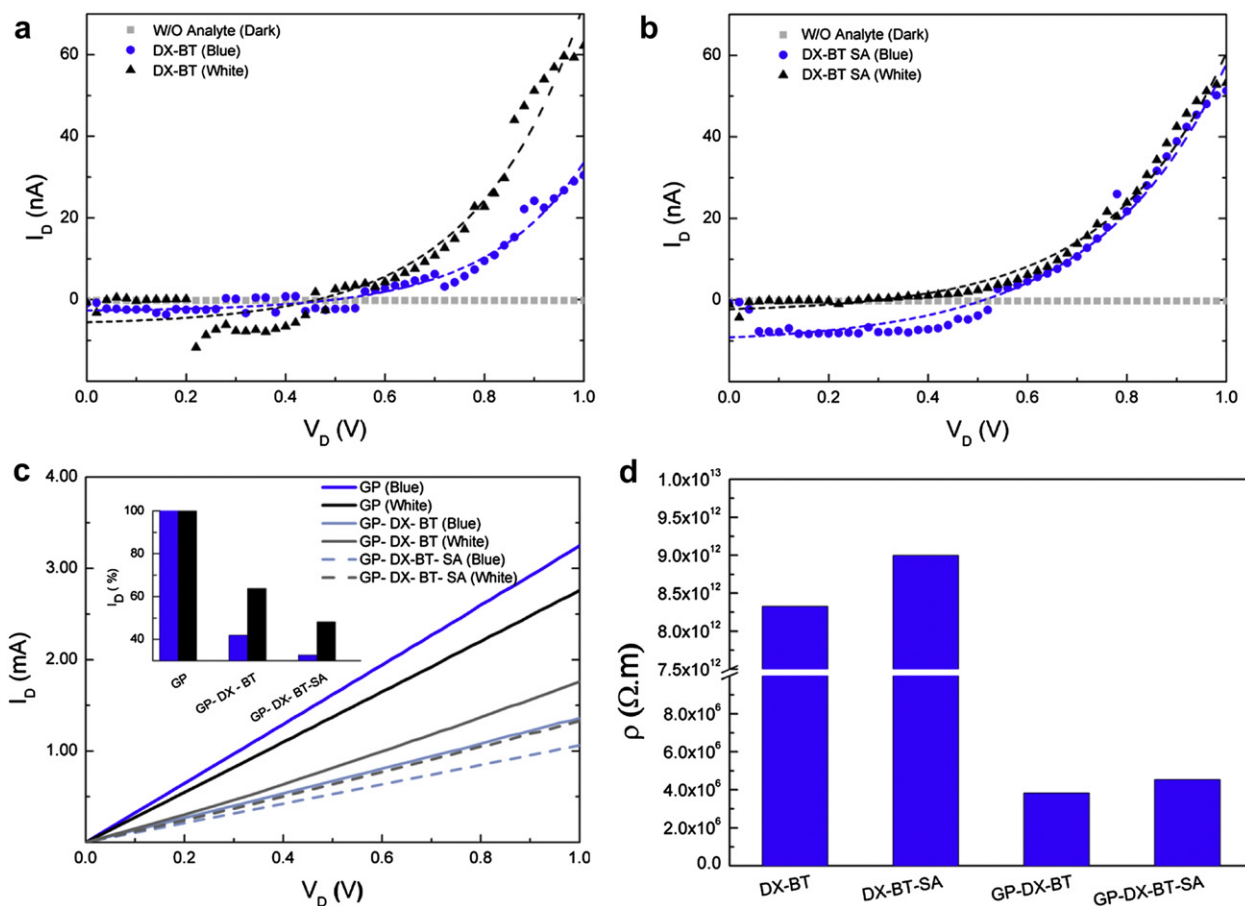


Fig. 2. The I – V characteristics of DX-BT nanostructures at $V_G = 0 \text{ V}$. (a) The I – V characteristics under optical excitation in DX-BT without a GP sheet for no light (square), blue light at 460 nm (circle) and white light at 400–800 nm (triangle). (b) The I – V behavior after the DX-BT lattice was functionalized with SA. An increase in current for blue light whereas a decrease in current for white light that features SA functionalization on DX-BT can be seen. (c) Light irradiation wavelength dependant I – V characteristics of DX-BT, DX-BT-SA with GPs. The significant increase in current from nanoampere to milliamperes is due to the graphene conductance. Decrease in current indicates graphene surface adsorbed DX-BT-SA. Inset shows the percentage current, 100% for GP itself, through the samples with GPs controlled by blue (blue bars) and white (black bars) lights. (d) The change in resistivity for blue light irradiation. There is significant change in resistivity in DX-BT-SA and GP-DX-BT-SA of the order of 10^6 due to the presence of the graphene. (For interpretation of the references to color in this figure legend, the reader is referred to the web version of this article.)

as 100%, after adding DX-BT the percentage change in current is approximately 60% for white light, and approximately 40% for blue as shown in Fig. 2(c), inset. However, after adding the SA protein the current is found to be further reduced due to the insulating electrical property of the SA protein.

The effect of gate bias voltage was also evaluated with an I – V evaluation for blue light as described in Fig. 3. GP shows minimal change in the drain current, I_D with respect to various gate bias voltages, $V_G = -30, -18, -6, +6, +18$ and 30 V as compared to the dark case and the blue light irradiated case, as depicted in Fig. 3(a) and (b), respectively. However after attachment of DX-BT onto GP, we observed a decrease in the response, specifically for the negative bias voltage regime as seen in Fig. 3(c). The transfer characteristics after the addition of SA caused change in I_D with an extensive gap for the negative V_G . These evaluations encouraged us to study the light dependant switching behavior of GP-DX-BT-SA. The photoisomerization of DNA nanostructures on the graphene surface provides a useful organic switch as shown in Fig. 4. The DX-BT lattice was exposed periodically to an optical input of blue light with a constant switching time. With an ON and OFF switching mode, we observed a linear increase and decrease in current. This switching action is swift and reversible with a constant change in current with the noticeable amplitude magnitude of about 0.05 mA. By use of the controlled electron fluctuations, highly reproducible supramolecular organic switching is achieved. Existing duplex DNA based switching devices already reversibly change the fluorescence [26], but 2D DNA lattice based optical switching will give us

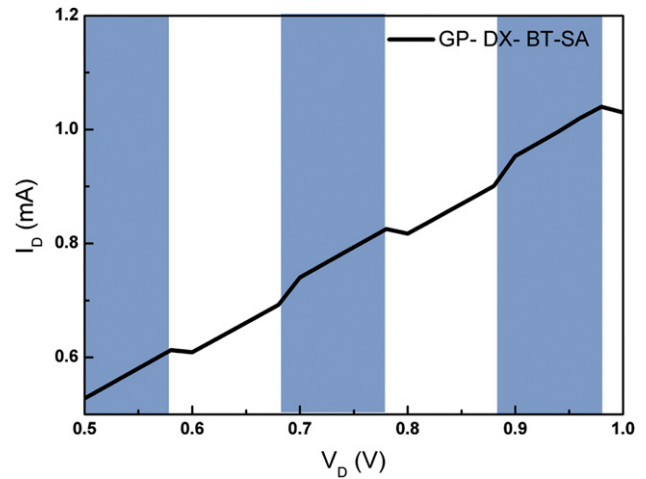


Fig. 4. Switching I – V response of GP-DX-BT-SA for the blue light irradiation where the significant switching action is reliable, reversible and fast. The switching current amplitude due to the blue light is about 0.05 mA. The blue regions indicate the ON signal with blue irradiation and the white shows the OFF signal. (For interpretation of the references to color in this figure legend, the reader is referred to the web version of this article.)

a controlled (by the amount of the DNA and their geometries), predictable (by the coverage rate control on the substrate between the electrodes) and efficient (comparing with existing biosensors) organic switch as well in sensor applications.

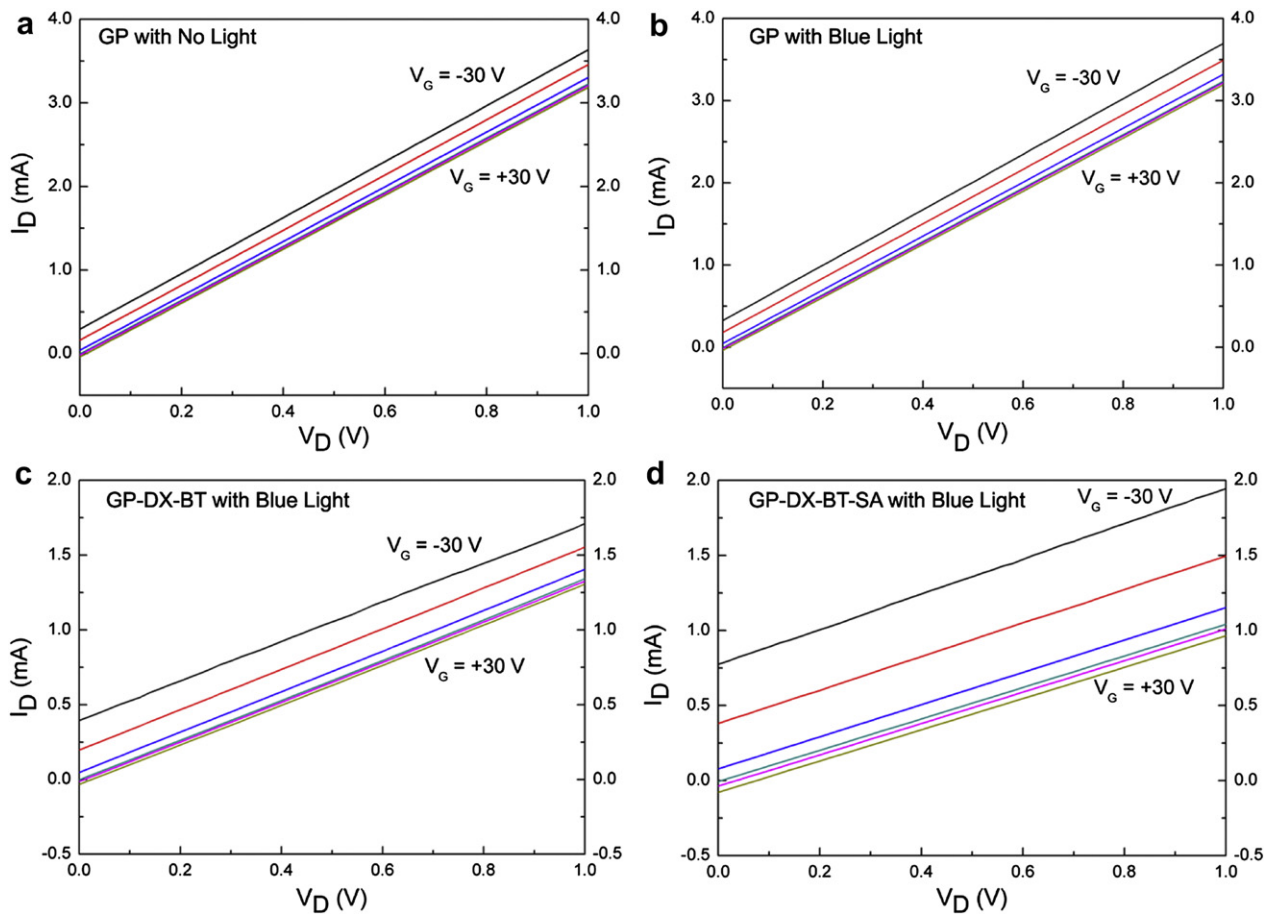


Fig. 3. The I – V characteristics of DX-BT lattices for blue light irradiation with 6 different gate voltages, $V_G = -30, -18, -6, +6, +18,$ and $+30$ V, from top to bottom shown in graphs. (a) The I – V response of GP for no light and without analyte. (b) The I – V response of GP after blue light irradiation. Minor variation in I_D is observed. (c) The I – V characteristic behavior when DX-BT is functionalized on GP for blue light. The I_D is found to be decreased as compared with GP only, with significant change in I_D especially for minus gate bias. (d) shows further enhancement in I_D for negative bias voltages when SA is added. (For interpretation of the references to color in this figure legend, the reader is referred to the web version of this article.)

Conventional optical techniques with biological materials have opened doors for interdisciplinary research and development in nano-bio sciences and technologies. Here we have demonstrated the photo-induction of electrons in 2D DNA lattices and its feasibility in organic switching with great sensitivity and reversibility. Consequently a 2D DNA lattice based nano-sensor is expected to have great potential for a number of applications, such as immunology, forensic science and toxin detection in the near future.

Acknowledgments

This research was supported by Basic Science Research Program through the National Foundation of Korea (NRF) funded by the Ministry of Education, Science and Technology (2010-0015035) to TK and by the Basic Science Research Program through the National Research Foundation of Korea (NRF) funded by the Ministry of Education, Science and Technology (2010-0013294) to SHP.

References

- [1] H.W. Liao, C.L. Nehl, J.H. Hafner, *Nanomedicine* 1 (2006) 201.
- [2] V. Berry, S. Rangaswamy, R.F. Saraf, *Nano Lett.* 4 (2004) 939.
- [3] V. Berry, R.F. Saraf, *Angew. Chem. Int. Ed.* 44 (2005) 6668.
- [4] H. Cai, X.N. Cao, Y. Jiang, P.G. He, Y.Z. Fang, *Anal. Bioanal. Chem.* 375 (2003) 287.
- [5] F. Patolsky, G.F. Zheng, C.M. Lieber, *Anal. Chem.* 78 (2006) 4260.
- [6] H. Cai, C. Xu, P.G. He, Y.Z. Fang, *J. Electroanal. Chem.* 510 (2001) 78.
- [7] J.D. Le, Y. Pinto, N.C. Seeman, K. Musier-Forsyth, T.A. Taton, R.A. Kiehl, *Nano Lett.* 4 (2004) 2343.
- [8] Y. Cui, Q.Q. Wei, H.K. Park, C.M. Lieber, *Science* 293 (2001) 1289.
- [9] H.M. So, D.-W. Park, E.-K. Jeon, Y.-H. Kim, C.-K. Lee, S.Y. Choi, S.C. Kim, H. Chang, J.-O. Lee, *Small* 4 (2008) 197.
- [10] J. Chen, N.C. Seeman, *Nature* 350 (1991) 631.
- [11] Y. Zhang, N.C. Seeman, *J. Am. Chem. Soc.* 116 (1994) 1661.
- [12] C. Mao, W. Sun, N.C. Seeman, *J. Am. Chem. Soc.* 121 (1999) 5437.
- [13] C. Mao, T.H. LaBean, J.H. Reif, N.C. Seeman, *Nature* 407 (2000) 493.
- [14] T.H. LaBean, H. Yan, J. Kopatsch, L. Furong, E. Winfree, J.H. Reif, N.C. Seeman, *J. Am. Chem. Soc.* 122 (2000) 1848.
- [15] H. Yan, S.H. Park, G. Finkelstein, J.H. Reif, T.H. LaBean, *Science* 301 (2003) 1882.
- [16] D. Liu, S.H. Park, J.H. Reif, T.H. LaBean, *Proc. Natl. Acad. Sci.* 101 (2004) 717.
- [17] S.H. Park, P. Yin, Y. Liu, J.H. Reif, T.H. LaBean, H. Yan, *Nano Lett.* 5 (2005) 729.
- [18] P.W.K. Rothmund, *Nature* 440 (2006) 297.
- [19] S. Hamada, S. Murata, *Angew. Chem. Int. Ed.* 121 (2009) 6952.
- [20] C.Y. Liang, E.G. Scalco, *Nature* 200 (1963) 1319.
- [21] K. Ijioa, T. Sawadaishib, M. Shimomuraab, *Mol. Crystals Liquid Crystals* 371 (2001) 375.
- [22] X.T. Gao, X. Fu, L.M. Mei, S.J. Xiea, *J. Chem. Phys.* 124 (2006) 234702.
- [23] E. Winfree, F.R. Liu, L.A. Wenzler, N.C. Seeman, *Nature* 394 (1998) 539.
- [24] X. Lv, Y. Huang, Z. Liu, J. Tian, Y. Wang, Y. Ma, J. Liang, S. Fu, X. Wan, Y. Chen, *Small* 5 (2009) 1682.
- [25] F.T. Vasko, V. Ryzhii, *Phys. Rev. B* 77 (2008) 195433.
- [26] S. Uno, C. Dohno, H. Bittermann, V.L. Malinovskii, R. Häner, K.A. Nakatani, *Angew. Chem. Int. Ed.* 48 (2009) 7362.